Environmental Research Letters

LETTER • OPEN ACCESS

Biogeophysical controls on soil-atmosphere thermal differences: implications on warming Arctic ecosystems

To cite this article: J Aalto *et al* 2018 *Environ. Res. Lett.* **13** 074003

IOP Publishing Environ. Res. Lett. 13 (2018) 074003 https://doi.org/10.1088/1748-9326/aac83e

Environmental Research Letters

LETTER

RECEIVED
17 January 2018

REVISED
30 April 2018

ACCEPTED FOR PUBLICATION
29 May 2018

PUBLISHED
26 June 2018

Biogeophysical controls on soil-atmosphere thermal differences: implications on warming Arctic ecosystems

J Aalto[1,2,6], D Scherrer[3], J Lenoir[4], A Guisan[3,5] and M Luoto[1]

1 Department of Geosciences and Geography, University of Helsinki, PO Box 64, Gustaf Hällströmin katu 2a, 00014 Helsinki, Finland
2 Finnish Meteorological Institute, PO Box 503, FI-00101 Helsinki, Finland
3 Department of Ecology and Evolution, University of Lausanne, CH-1015 Lausanne, Switzerland
4 UR Ecologie et dynamique des systèmes anthropisés (EDYSAN, UMR 7058 CNRS-UPJV), Université de Picardie Jules Verne, 1 rue des Louvels, FR-80000 Amiens, France
5 Institute of Earth Surface Dynamics, University of Lausanne, CH-1015 Lausanne, Switzerland
6 Author to whom any correspondence should be addressed.

E-mail: juha.aalto@helsinki.fi

Keywords: thermal variability, microclimate, soil-atmosphere decoupling, soil temperature, structural equation model, snow cover, offset

Supplementary material for this article is available online

Abstract

Soil temperature (ST) has a key role in Arctic ecosystem functioning and global environmental change. However, soil thermal conditions do not necessarily follow synoptic temperature variations. This is because local biogeophysical processes can lead to a pronounced soil-atmosphere thermal offset (ΔT) while altering the coupling (βT) between ST and ambient air temperature (AAT). Here, we aim to uncover the spatiotemporal variation in these parameters and identify their main environmental drivers. By deploying a unique network of 322 temperature loggers and surveying biogeophysical processes across an Arctic landscape, we found that the spatial variation in ΔT during the AAT$\leq$0 period (mean $\Delta T = 6.0\,°\mathrm{C}$, standard deviation $\pm\,1.2\,°\mathrm{C}$) was directly and indirectly constrained by local topography controlling snow depth. By contrast, during the AAT>0 period, ΔT was controlled by soil characteristics, vegetation and solar radiation ($\Delta T = -0.6\,°\mathrm{C} \pm 1.0\,°\mathrm{C}$). Importantly, ΔT was not constant throughout the seasons reflecting the influence of βT on the rate of local soil warming being stronger after (mean $\beta T = 0.8 \pm 0.1$) than before ($\beta T = 0.2 \pm 0.2$) snowmelt. Our results highlight the need for continuous microclimatic and local environmental monitoring, and suggest a potential for large buffering and non-uniform warming of snow-dominated Arctic ecosystems under projected temperature increase.

1. Introduction

In the Arctic, climate is warming at twice the rate as lower latitudes, and where the increase in synoptic temperature might have a strong effect on near-surface thermal conditions (Post *et al* 2009, IPCC 2013). Soil temperature (ST) is fundamentally linked to various aspects of ecosystem functioning, plant growth and reproduction (Bowman and Seastedt 2001, Körner 2003), soil biogeochemistry (nutrient enrichment and microbial activity; Starr *et al* 2008, Saito *et al* 2009) and frost-related geomorphological processes (French 2007). Alterations in the topsoil thermal regime were shown to directly modify ecosystem dynamics through changes in both resources and disturbances (Pearson *et al* 2013, le Roux and Luoto 2014, Paradis *et al* 2016) and feedback on climate itself either through permafrost degradation and methane release (Blok *et al* 2011) or through plant redistribution and changes in albedo (Pearson *et al* 2013, Pecl *et al* 2017). However, near-surface thermal conditions do not necessarily follow synoptic temperature variations (Geiger *et al* 2009), with consequences for biotic and abiotic responses to climate warming (Lawrence and Swenson 2011, Lenoir *et al* 2017). While near-surface soil and air temperatures generally respond to temporal fluctuations in ambient air temperature (AAT) (Pollack *et al* 2005), locally they can substantially differ due to effects of both physiographic and biophysical processes (Körner 2003, Dobrowski 2011, Lenoir *et al* 2017)

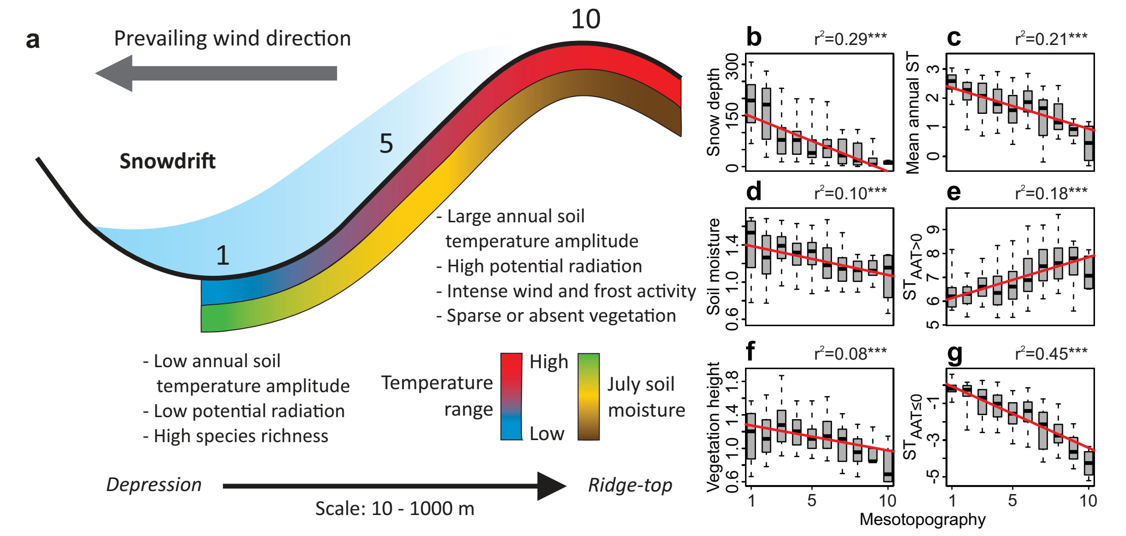

Figure 1. General variation in ST and moisture conditions along the mesotopographical gradient (estimated on a ten-point scale) (*a*) from a local depression (1), mid-slope (5) to a ridge top (10). In the sub-panels, mesotopography was contrasted against: (*b*) snow depth (cm); (*c*) mean annual ST (ST, °C); (*d*) soil moisture (% volumetric water content, VWC); (*e*) mean summer (June–August) ST (°C); (*f*) maximum vegetation height (cm); and (*g*) mean winter ST (°C). The boxplots present median, 1st and 3rd quartiles and 95% range of variation of 322 loggers, while the red line depicts the fitted linear function. The amount of variance explained by the fitted function is expressed as adjusted r-squared (r^2) values. Statistical significance of the fit is indicated as *** = $p \leq 0.001$. Note the logarithmic scales in panels (*d*) and (*f*).

with ST being even more buffered than near-surface air temperature, especially under low vapor pressure deficit (Ashcroft and Gollan 2013). Considering the key role of ST in Arctic ecosystems, such differences may have important consequences on climate feedbacks, but up to now our knowledge of spatiotemporal links between soil and AATs have remained limited. Quantifying the magnitude of the difference between soil and ambient air temperatures and most importantly the biogeophysical processes underlying is necessary to improve projections of changes in STs under anthropogenic climate change, and its subsequent impact on biodiversity redistribution in Arctic ecosystems.

Earlier studies have documented extreme fine-scale variation of ST in Arctic-alpine systems (Scherrer and Körner 2010, Aalto *et al* 2013). Such soil microclimatic mosaic is attributable to local variation in biogeophysical conditions such as topography, surface soil characteristics and vegetation (Wundram *et al* 2010, Ashcroft and Gollan 2013, Graae *et al* 2018). Environmental heterogeneity in these systems is chiefly a direct, as well as an indirect, consequence of local topography (i.e. the mesotopographical depression-ridge-top continuum), controlling snow distribution, snow depth and subsequently soil moisture and vegetation (Billings 1973, Bruun *et al* 2006, le Roux *et al* 2013a) (figure 1(*a*)). Similarly, these factors can be expected to drive the instantaneous soil-atmosphere thermal offset (i.e. the difference between ST and AATs ΔT = ST − AAT; figure 2). For example, ST variations under a thick insulating snow pack are greatly reduced (Grundstein *et al* 2005), whereas dry soils on wind-exposed ridges abruptly respond to changes in AAT throughout the year due to high vapor pressure deficit (Graham *et al* 2012, Ashcroft and Gollan 2013). Therefore ΔT can provide an indication of the strength of the 'biogeophysical processes' that mediate AAT and create a heterogeneous soil thermal mosaic over the Arctic landscape (Scherrer and Körner 2010, 2011, Lenoir *et al* 2013).

In recent years, there were attempts to integrate this microclimatic variation into coarse-grained macroclimatic grids by using thermal variability within a spatial unit (e.g. 1 km^2) as a proxy for the landscape's potential to buffer against climate warming (Scherrer and Körner 2010, 2011, Lenoir *et al* 2013). Such an approach can provide an indication of climate resilience or potential for microrefugia (Patsiou *et al* 2014). However, the general idea of fine-grained and short-distance thermal variability exceeding projected temperature change will allow living organisms to persist within the landscape (Graae *et al* 2018) does not provide understanding of the environmental factors generating this buffering effect. Another key process involved in macroclimate buffering is the thermal coupling between interior (here soil microclimate) and exterior (i.e. macroclimate or synoptic) conditions (Lenoir *et al* 2017). Similarly to ΔT, soil-atmosphere thermal coupling, which is the slope parameter of the relationship between AAT and ST (βT; figure 2), is likely to be affected by the local biogeophysical conditions. This suggests that parts of the Arctic landscape can be climatically more stable over time (i.e. more decoupled, low βT values) than others, leading to a spatially uneven local response to changes in macroclimatic forcing. An analysis of time series in combination with direct field measurements of

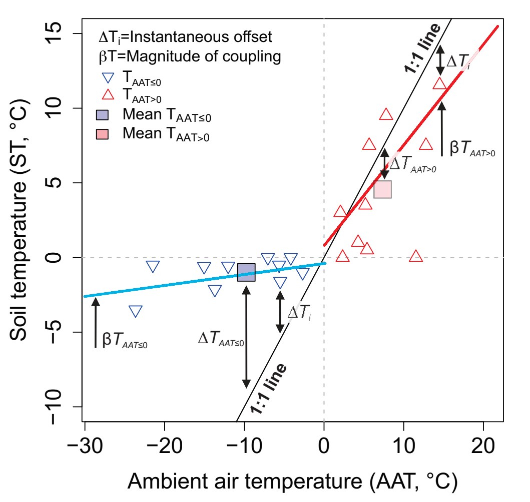

Figure 2. Derivation of instantaneous and intra-seasonal soil (ST) - air temperature (AAT) offset (ΔT) and coupling (βT). For the sake of clarity, only a random sample of 10 seasonal ST/AAT values (the symbols) were plotted here from a logger located in the North Site (grid 2; see figure 3 for details). The light blue and red lines depict the piecewise ordinary least-square (OLS) regression functions for the AAT ≤ 0 °C and AAT > 0 °C periods, respectively. Both OLS and mean values (colored boxes) are based on all seasonal measurements of the logger.

topography, soil and vegetation can provide new insights into the current magnitudes of ΔT and βT and thus the buffering potential in Arctic landscapes.

Here, by using data from a unique network of 322 temperature loggers and climate stations we aim to: (1) uncover the spatiotemporal variation of soil-atmosphere offset (ΔT) and coupling (βT) parameters within a topographically complex Arctic landscape; (2) identify the main biogeophysical drivers behind ΔT and βT using field-quantified environmental data within a structural equation modelling (SEM) framework; and (3) use measures of βT to explore the current buffering potential of these topographically rich landscapes in respect to projected climate warming.

2. Materials and methods

2.1. Study site and sampling design

The study was conducted in five sites located within the Saana mountain range in northwestern Finnish Lapland (ca. 69°N, 21°E; figure 3). The sites were located at ca. 600–800 m a.s.l. with different aspects and above the natural treeline (~150 m a.s.l.) formed by mountain birch (*Betula pubescens* ssp. *czerepanovii*). Mean annual, January and July air temperatures measured at the nearby Kilpisjärvi meteorological station (69°02'N, 20°47'E, 480 m a.s.l., ca. 1.5 km away) over the period 1981–2010 were −1.9 °C, −12.9 °C and 11.2 °C, respectively. Mean annual precipitation sum was 487 mm over the same period (Pirinen *et al* 2012). Synoptic temperatures recorded during the study period (2013–2014) were representative of the average conditions during 1981–2010 (figure S1 available at stacks.iop.org/ERL/13/074003/mmedia), while some unusually warm days (i.e. mean daily temperature exceeding the 87.5th percentile of 1981–2010) were observed in August and September 2013. On average, the seasonal snow cover persists until late June (starting from late September) with over 225 days of snow cover. Conditions are favorable for the occurrence of discontinuous/sporadic permafrost (Gisnås *et al* 2016), although King and Seppälä (1987) showed that the permafrost in this area is likely to be a relict, as shown by the permafrost table being located deeper than 10 m below the soil surface. One can thus reasonably assume that the permafrost is not affecting thermal-hydrological conditions of the topsoil. The study area is topographically complex with surface terrain alternating from local depressions to ridges within distances of tens of meters. The soils consist mainly of glacigenic till deposits, but depending on local topography, bare rocks (summits and steep slopes) and thin organic soils (depressions) are also abundant. The vegetation in the study area is characteristic of Arctic-alpine tundra dominated by shrubs (e.g. *Empetrum nigrum* ssp. *hermaphroditum*, *Betula nana*), graminoids (e.g. *Deschampsia flexuosa*, *Carex bigelowii*), mosses (e.g. *Dicranum fuscescens*) and lichens (e.g. *Ochrolechia frigida*) with boreal features at lower elevations (le Roux *et al* 2013b).

For the subsequent analyses, a total of 21 grids (8 m × 20 m, each consisting of 160 adjacent 1 m^2 grid cells) were deployed across the five study sites (three on Low, West and High sites, and six on both North and South sites; figure 3). Such a setup was chosen to systematically cover a wide range of environmental conditions, particularly focusing on mesotopography (figure 1(*a*)). Grids covered 0.34 ha and the distance between the grids varies from ca. 40 m to 3.2 km, with the median distance being 713 m.

2.2. Soil and ambient air temperature data

We recorded annual soil temperature (ST) within each of the 21 grids by using iButton temperature loggers (Thermochron iButton® DS1291G; Dallas Maxim; with a temperature range between −40 °C and 85 °C, resolution of 0.5 °C and accuracy of 1.0 °C). The loggers (originally 378 units) were placed across each study grid at 10 cm below ground and at 4 m intervals (with a total of 18 loggers per study grid; figure 3). Mean horizontal distance between the loggers across the sites varied from 53 m–126 m. Due to technical malfunctions and displacements, only the data from 322 loggers could be retrieved over the studied time period. Loggers recorded STs every four hours from 26 June 2013–25 June 2014.

AAT data (from June 2013–June 2014) were retrieved from two meteorological stations operated by the Finnish Meteorological Institute and located in the vicinity of the study sites (Kilpisjärvi Kyläkeskus

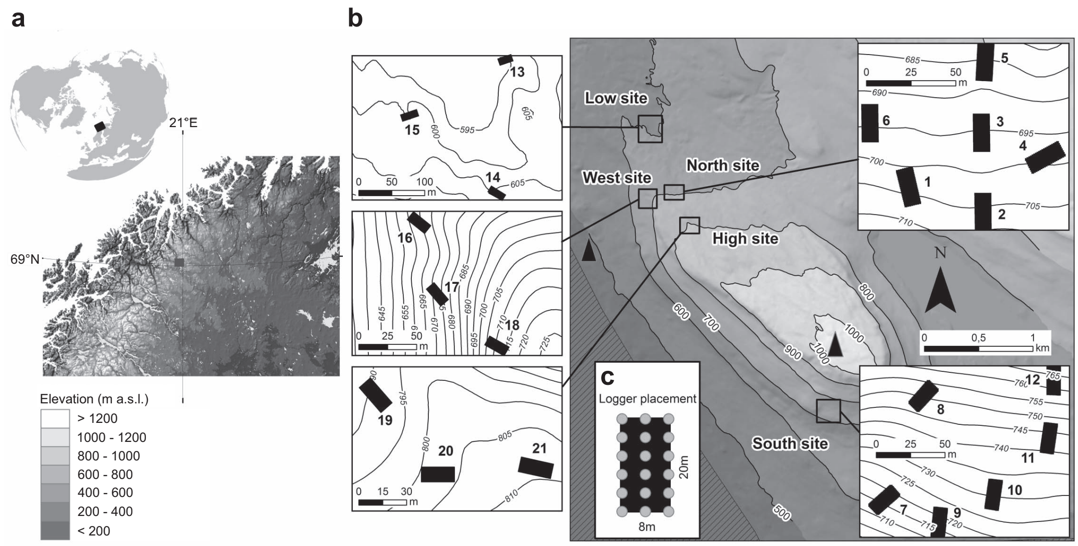

Figure 3. Location of the study area in high-latitude Fennoscandia. Panels *a* and *b* show the locations of the 21 study grids (8 m × 20 m) across the Saana mountain range, Kilpisjärvi. The positions of the two meteorological stations (MET1, 480 m a.s.l.; MET2, 1009 m a.s.l.) are indicated with black triangles. Panel *c* shows a schematics of the logger placement (grey circles) at four meter interval in each grid (number of loggers per grid = 18).

meteorological station [MET1], 69°02'N, 20°47'E, 480 m a.s.l. and Saana meteorological station [MET2] 69°2'N, 20°51'E, 1002 m a.s.l.; figure 3).

To characterize the ST regime within the study area, three ST-derived variables were calculated from the time series: annual mean ST (ST_{annual}); mean ST over the period with below freezing point AAT (AAT ≤ 0, on average covering 60% of the instantaneous ST measurements); and mean ST over the period with above freezing point AAT (AAT > 0). These two seasons separated by the phase-change point of water intuitively depict a transition from atmospheric conditions favoring snow accumulation and melting. For our definition, these two periods were not limited to consecutive time steps.

2.3. Calculation of the soil-atmosphere thermal offset

The assessment of the soil-atmosphere thermal offset (ΔT) included several steps: (1) the instantaneous (i.e. at every time step) AAT lapse rate was determined by calculating the temperature difference between the two meteorological stations (i.e. MET1 and MET2; average difference = −1.8 °C; 90% range of variation = [−9.2; 9.9 °C]); (2) the obtained AAT difference was divided by the 522 m elevation gradient separating the two stations; (3) the AAT for the logger sites were determined based on the instantaneous lapse rate and the average altitude of each grid; and (4) the instantaneous thermal offset ($\Delta T_i = ST_i - AAT_i$) was calculated for each logger at 4 hour time intervals. Missing values (2% of the annual series) were introduced to the ΔT_i time series due to absent hourly AAT recordings, and were excluded from subsequent analyses. Finally, the ΔT_i were averaged to obtain mean values for two periods (figure 2): AAT ≤ 0 (i.e. $\Delta T_{AAT\leq 0}$) and AAT > 0 (i.e. $\Delta T_{AAT>0}$).

2.4. Calculation of the soil-atmosphere thermal coupling

Following Lenoir *et al* (2017), we measured the soil-atmosphere thermal coupling (βT) by running an ordinary least-square (OLS) regression, where STs of each logger were regressed against AATs (figure 2). However, due to the strong influence of snow depth on STs, we used a piecewise OLS regression approach (Toms and Lesperance 2003) by splitting the annual time series into two distinct seasons: (1) AAT ≤ 0 (i.e. $\beta T_{AAT\leq 0}$); and (2) AAT > 0 (i.e. $\beta T_{AAT>0}$). The resulting slope estimates indicate the agreement between the ST and AAT time series with values close to 1 indicating strong coupling and thus low decoupling.

2.5. Environmental variables

Volumetric soil moisture was measured in all grid cells during the middle of the growing season (16 July 2013) within a time-window of 48 consecutive hours without precipitation using a hand-held time-domain reflectometry sensor (FieldScout TDR 300; Spectrum Technologies, Plainfield, IL, USA) up to a depth of 10 cm, taking the mean of ca. 3 measurements per grid cell (Aalto *et al* 2013). A recent study by le Roux *et al* (2013a) indicates that spatial patterns of soil moisture remain relatively constant within and between the growing seasons (Pearson's correlations of repeated measurements > 0.85), thus justifying our use of single measurements in subsequent analyses.

Potential incoming solar radiation (PISR) for both seasons (AAT ≤ 0 [~October–May] and AAT > 0 [~May–October]; MJ cm^{-2}; assuming clear sky conditions) was calculated for each grid cell using the 'Points Solar Radiation' tool in ArcGis 10.3. While the elevation of each grid cell was estimated from a digital elevation model (10 m × 10 m; provided by the National Land Survey of Finland), slope angle and aspect values were measured in the field.

At each grid cell, mesotopography (i.e. a measure of local topography; Billings 1973) was estimated on a 10 point scale (1 = depressions, 5 = mid-slopes, 10 = ridge tops; figure 1(*a*)). Snow depth (cm) was manually recorded by installing plastic tubes across the study grids at the end of the growing season, which were subsequently measured during the period of maximum snow cover (March 2014). Maximum vegetation height data were collected in July 2011–2013, during the peak of the growing season. Peat depth represents the thickness of the organic layer and was determined by means of three measurements inside each grid cell, using a thin metal rod to probe the soil (Rose and Malanson 2012). Cover of rock represents the percentage of bare rock and coarse gravel within each grid cell.

2.6. Estimation of the landscape's current buffering potential

To explore the potential impact of the current soil-atmosphere βT on STs under warming conditions, we first shifted the seasonal STs according to an AAT warming of +5 °C (i.e. unbuffered ST in equation (1), corresponding to the RCP8.5 emission pathway for the time slice of 2070–2099). Then, βT values were used to multiply the unbuffered ST projections to obtain buffered STs under +5 °C AAT warming (Lenoir *et al* 2017). Finally, the amount of thermal buffering (k) accounting for decoupling effect between current and future conditions was measured as a relative proportion using the following formula:

$$k = 1 - \left(\frac{\bar{x}_{\text{buffered ST}} - \bar{x}_{\text{observed ST}}}{\bar{x}_{\text{unbuffered ST}} - \bar{x}_{\text{observed ST}}}\right) \quad (1)$$

where $\bar{x}$ is the arithmetic mean. Thus, a k value close to zero indicates low buffering potential, while a k value close to one suggests a strong buffering potential.

In addition to assess the current buffering potential, we estimated k for AAT ≤ 0 in respect to two alternative scenarios where current snow depths were altered by +50 cm (excluding ridge areas affected by wind transportation) and −50 cm (assuming +5 °C AAT warming). Whereas future increase in water precipitation (and thus less snow accumulation) is commonly expected (Bintanja and Andry 2017), we also examined a possibility for increasing snow depth (i.e. +50 cm scenario), which has been observed in parts of the Arctic (Callaghan *et al* 2011). We predicted average $\beta T_{\text{AAT}\leq 0}$ values at the different snow depth scenarios based on an empirical function ($\beta T_{\text{AAT}\leq 0} = e^{-0.99-0.01\times \text{snow depth}}$). The current $\beta T_{\text{AAT}\leq 0}$ values were adjusted by the average changes in βT when comparing a snow-depth alteration scenario to current conditions. Finally, the k value for a given snow-depth alteration scenario was re-calculated based on the adjusted βT values.

2.7. Statistical analyses

Prior to any statistical analysis, snow depth, rock cover, peat depth, vegetation height and soil moisture variables were log-transformed to approximate normal distributions. The spatial variation in ΔT and βT was related to this list of environmental variables using a structural equation modeling (SEM) framework based on path models (Grace 2006), here as implemented in the R package 'piecewiseSEM', version 1.1.3 Lefcheck (2015). SEM is a statistical modeling technique that combines pathways of multiple predictor and response variables in a single network (Grace 2006). An important difference compared to traditional multiple regression is that, in SEM, variables can appear as both predictors and responses (i.e. endogenous variables), thus allowing for investigation of indirect, mediating or cascading effects (Lefcheck 2015) (figure S2).

Due to the non-independent spatial structure in the data (figure 3), the component models were fitted as linear mixed-effect models (LMMs) using attributes 'Site' and 'Grid' as nested random intercept factors (Bates *et al* 2014). None of the component models were confounded by multicollinearity as indicated by low variance inflation factor (VIF<2; 'vif' function from the R package 'car', version 2.1–3; Fox and Weisberg 2011). The goodness-of-fit of the SEMs were evaluated using Fisher's *C*, where *p*-values for the chi-square > 0.05 indicates a model consistent with the observations (Lefcheck 2015).

The modelling was initiated by defining a full model representing hypothetical causal pathways from the exogenous variables (mesotopography, radiation, and rock cover), through mediators or endogenous variables (snow depth, soil moisture and vegetation) to the response variables (i.e. seasonal ΔT and βT). For $\Delta T_{\text{AAT}\leq 0}$ and $\beta T_{\text{AAT}\leq 0}$, the effect of $\text{PISR}_{\text{AAT}\leq 0}$ was not tested due to low direct solar radiations at high latitudes during polar nights that prevails during most of the AAT ≤ 0 period. An error covariance term was defined between peat depth and soil moisture since soil moisture is strongly affected by peat depth. To calibrate each component model, we iteratively (starting from the full model) excluded the most insignificant variable from the models until only significant terms remained (Taka *et al* 2016). According to Fisher's *C* statistics, all SEMs provided an adequate fit to the data with $C_8 = 8.47$ ($p = 0.39$) and $C_{12} = 10.44$ ($p = 0.58$) for $\Delta T_{\text{AAT}\leq 0}$ and $\Delta T_{\text{AAT}>0}$, respectively. For $\beta T_{\text{AAT}\leq 0}$ and $\beta T_{\text{AAT}>0}$, the corresponding statistics were $C_8 = 9.24$ ($p = 0.32$) and $C_6 = 6.98$ ($p = 0.32$), respectively.

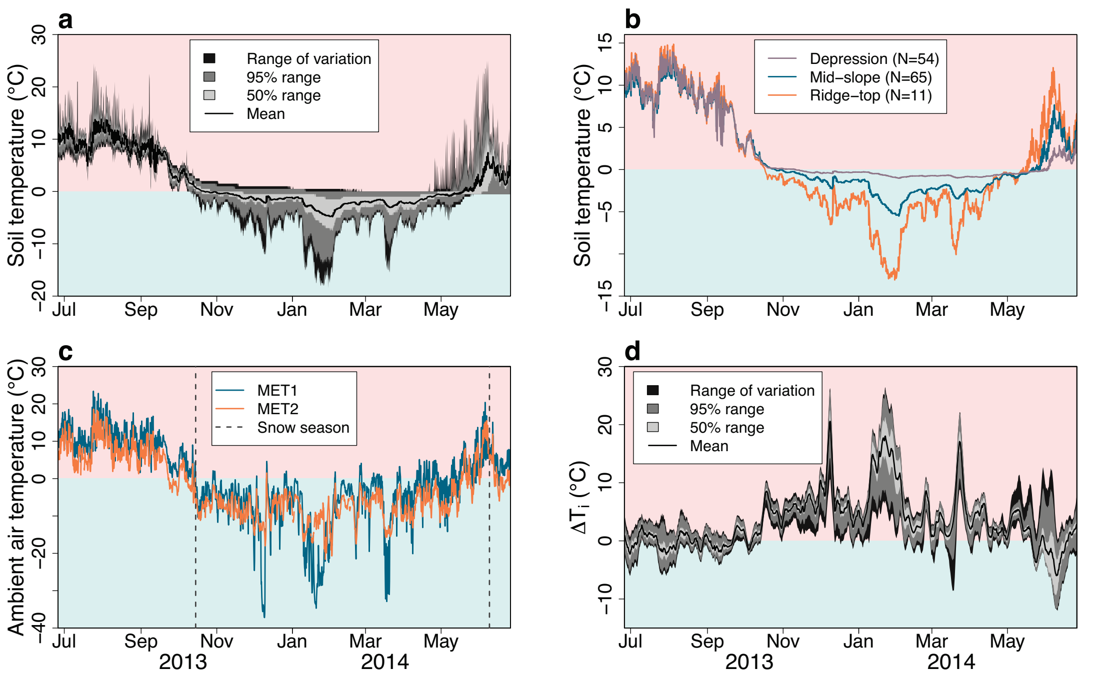

Figure 4. Temporal variation in soil and air temperatures, and instantaneous soil-atmosphere thermal offset. Panel (*a*) shows temporal fluctuation in the annual soil temperature (ST) series with mean (black line), 50%, 95% and absolute ranges (shaded grey-scale polygons). In (*b*), temporal variation in STs is averaged over three mesotopography levels: depression = 1–2 (mean snow depth = 165 cm); mid-slope = 5 (mean snow depth = 59 cm); and ridge-top = 9–10 (mean snow depth = 19 cm). Panel (*c*) shows ambient air temperature (AAT) measured at two nearby meteorological stations (MET1 [480 m a.s.l.] and MET2 [1002 m a.s.l.]), and the length of the permanent snow cover measured at MET1 (237 consecutive days with snow ≥ 1 cm, dashed lines). Panel (*d*) shows temporal variation in instantaneous ST-AAT offset (ΔT_i), smoothed using a two-day running mean filter for clarity. The ST data are based on four-hour interval records of temperature for each logger ($N = 322$) and over a period of one year (from 26 June 2013–25 June 2014). N = number of loggers.

3. Results

Our data revealed remarkable temporal (figure 4) and spatial (figures 1(*b*)–(*g*); tables 1–S1) variations in STs and biogeophysical variables. For example, snow depth was found to vary at most 256 cm and soil moisture 42 % VWC between adjacent logger locations (figure S3(*a*)). During AAT > 0, STs generally followed AATs, being slightly cooler on average (mean $\Delta T_{AAT>0} = -0.6$ °C). However, during AAT ≤ 0, the pattern differed, with STs being, on average, much warmer than AATs (mean $\Delta T_{AAT\leq 0} = 6.0$ °C). Similar to absolute STs, notable intra-grid spatial variation in ΔT was observed (figure S3(*b*); table S2). During AAT > 0, STs were, on average, closely coupled with AATs with βT ranging from 0.50–1.10, while under AAT≤0, βT ranged from 0.01–0.73. The intra-grid spatial variation in $\beta T_{AAT\leq 0}$ and $\beta T_{AAT>0}$ closely followed the relative patterns found for ΔT (table S2). Both $\Delta T_{AAT\leq 0}$ and $\beta T_{AAT\leq 0}$ showed strong and non-linear relationships with snow depth (figure 5).

Path models revealed season-specific networks of factors controlling ΔT (figures 6(*a*)–(*b*); figure S4). Mesotopography was found to directly and indirectly control $\Delta T_{AAT\leq 0}$ through a strong control on snow depth (standardized path coefficient = −0.52) which strengthened the effect of mesotopography on $\Delta T_{AAT\leq 0}$ (direct effect of snow depth = 0.30, net effect of mesotopography = −0.65). The factors directly

Table 1. Summary statistics ($N = 322$) for soil temperature (ST), soil-atmosphere thermal offset (ΔT) and coupling (βT) parameters as well as for several environmental variables. AAT = ambient air temperature, PISR = potential incoming solar radiation, SD = standard deviation, Min = minimum, Max = maximum, VWC = volumetric water content, mesotopo = mesotopography.

Variable	Unit	Mean	SD	Min	Max
Soil temperature					
ST_{annual}	°C	1.8	0.7	−0.4	3.4
$ST_{AAT\leq 0}$	°C	−1.5	1.2	−5.3	0.7
$ST_{AAT>0}$	°C	6.8	0.9	5.2	9.7
Soil-atmosphere thermal offset					
$\Delta T_{AAT\leq 0}$	°C	6.0	1.2	2.5	8.2
$\Delta T_{AAT>0}$	°C	−0.6	1.0	−2.2	2.3
Soil-atmosphere thermal coupling					
$\beta T_{AAT\leq 0}$	Unitless	0.20	0.15	0.00	0.73
$\beta T_{AAT>0}$	Unitless	0.84	0.10	0.59	1.10
Environmental variables					
Mesotopo	Index	5	2	1	10
Rock cover	% m^{-2}	12	19	0	94
$PISR_{AAT\leq 0}$	MJ cm^{-2}	0.008	0.004	0.000	0.014
$PISR_{AAT>0}$	MJ cm^{-2}	0.023	0.008	0.004	0.034
Soil moisture	% VWC	21	11	4	56
Snow depth	cm	80	69	0	319
Vegetation height	cm	17	11	4	80
Peat depth	cm	5	4	0	24

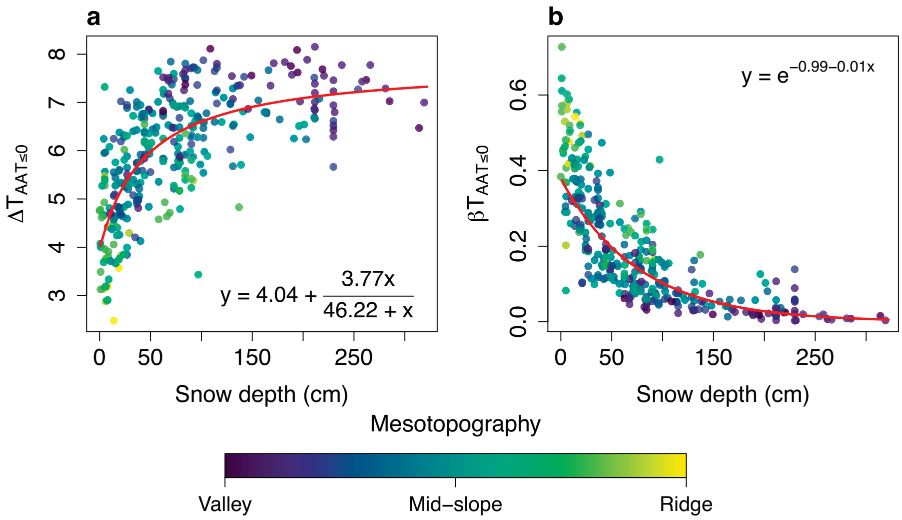

Figure 5. The relationship between snow depth (x-axis) and the soil-atmosphere thermal offset ((a), $\Delta T_{AAT\leq0}$ °C) or coupling ((b), $\beta T_{AAT\leq0}$) parameters (y-axis). The colors represent the loggers' location along mesotopographical gradient from a local depression (purplish colors), mid-slope (greenish colors) to a ridge top (yellowish colors). The red lines depict the fitted non-linear functions. AAT = ambient air temperature.

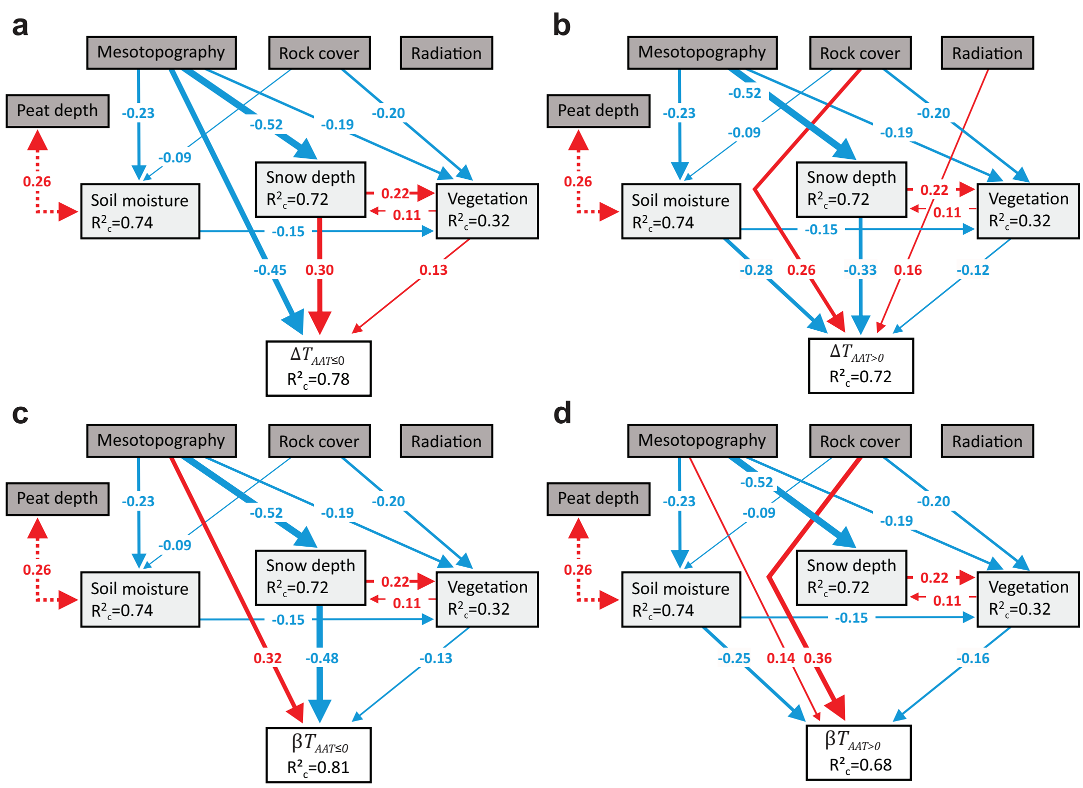

Figure 6. The environmental factors determining the soil-atmosphere thermal offset (ΔT) and coupling (βT) processes in the Arctic. For each structural equation model ((a)–(b), for $\Delta T_{AAT\leq0}$ and $\Delta T_{AAT>0}$, respectively; (c)–(d), for $\beta T_{AAT\leq0}$ and $\beta T_{AAT>0}$, respectively), only statistically significant paths are presented with their standardized path coefficients placed on the arrows. The thickness of the arrows is proportional to the strength of the relationships among variables (red for positive effect, blue for negative effect). The dashed line between the variables peat depth and soil moisture indicates error covariance. The amount of explained variance for component models is reported as conditional R^2_c based on the variance of both fixed and random terms. AAT = ambient air temperature.

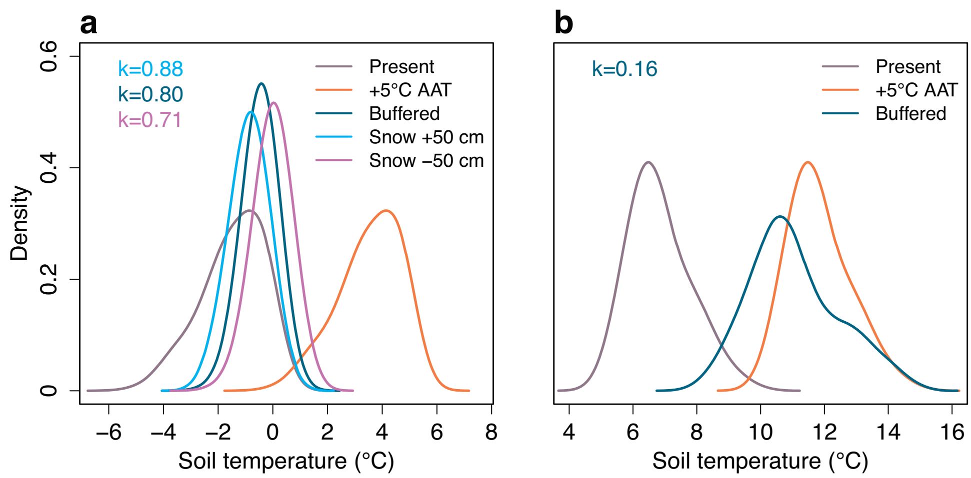

Figure 7. The current and projected (under several scenario of changes in temperature and snow depth conditions) thermal buffering potential (k) of an Arctic landscape. The kernel density functions (bandwidth = 0.5) depict the present condition, the unbuffered prediction (+5 °C AAT warming, corresponding to the outcome of emission scenario RCP 8.5 for 2070–2099 across the study area) and the buffered predictions (i.e. predicted future distribution adjusted by soil-atmosphere thermal coupling βT) in soil temperatures (STs) for two seasons: AAT $\leq$ 0 °C (*a*) and AAT > 0 °C (*b*). In addition, for AAT$\leq$0 °C the buffering potential was estimated under two snow-depth alteration scenarios, where observed snow depths were modified by +50 cm and −50 cm, respectively.

influencing $\Delta T_{\mathrm{AAT}>0}$ were more versatile with snow depth (−0.33; indicating the presence of late-lying/perennial snow), soil moisture (−0.28), and vegetation height (−0.12) having a negative effect while rock cover (0.28, partly controlling soil moisture) and potential solar radiation (0.16) having a positive effect. Although no direct effect of mesotopography on $\Delta T_{\mathrm{AAT}>0}$ was found, the net effect was clearly positive (0.21).

During AAT $\leq$ 0, the network of factors controlling soil-atmosphere thermal coupling ($\beta T_{\mathrm{AAT}\leq 0}$) resembled $\Delta T_{\mathrm{AAT}\leq 0}$ with the difference that the direct effect of snow depth was stronger (−0.48) and the direct effect of mesotopography weaker (0.32; figures 6(*c*)–(*d*); figure S5). During AAT > 0, rock cover showed the strongest direct effect on $\beta T_{\mathrm{AAT}>0}$ (0.36). In addition, $\beta T_{\mathrm{AAT}>0}$ was negatively linked to soil moisture (−0.25) and vegetation (−0.16). Although no significant effect of solar radiation was detected, $\beta T_{\mathrm{AAT}>0}$ was found to be directly controlled by mesotopography (0.14; in contrast to $\Delta T_{\mathrm{AAT}>0}$).

4. Discussion

Our results provide new insights into the factors determining ST in the Arctic throughout a complex network of biogeophysical processes affecting soil-atmosphere thermal offset (ΔT) and coupling (βT). Our study highlights the underestimated thermal variability available across very short spatial distances within Arctic ecosystems, supporting former work on the relevance of small-scale spatial variability in near-surface soil and air temperatures for biotic and abiotic responses under contemporary climate change (Scherrer and Körner 2010, Etzelmüller 2013, Lenoir *et al* 2013). The data suggest that local topography is a key factor directly (or indirectly throughout the mediating effect of e.g. snow depth) controlling the magnitude of the soil-atmosphere ΔT and βT. Despite the strong influence of snow on ΔT and βT in these systems, multiple other factors contributed to explain ΔT and βT during AAT > 0. For example, the effect of rock cover on ΔT and βT was notable, suggesting rock thermal conductivity to cause a strong coupling of ST with AAT in the topsoil. During warm periods, the excessive heating of rocky surfaces under strong solar radiation can lead to soils being warmer than AAT (i.e. βT >1) with the heat transfer function being reversed (ST warms AAT). In addition, our study confirms the role of soil moisture and vegetation as biogeophysical factors generally smoothing the spatiotemporal variation in STs (through e.g. thermal inertia and reduced net radiation fluxes) leading to notable soil-atmosphere ΔT and βT (Dobrowski 2011, Ashcroft and Gollan 2013).

Our findings suggest that the microclimatic response to meso- and macroclimatic forcing is likely to be altered by biogeophysical processes possibly leading to a non-uniform spatiotemporal soil warming with climate change. We assume that STs under snow cover should, on average, only be slightly affected by changes in AATs, because the very low coupling between soil and air temperatures during that period enhances the buffering potential of the landscape (k = 0.80; figure 7(*a*)). During AAT > 0, we assume that the average buffering potential should decrease relative to AAT $\leq$ 0 (k = 0.16) with STs being more coupled with AATs (figure 7(*b*)).Environmental heterogeneity will cause this buffering potential to substantially vary over the study area (figure S6). Assuming a +5 °C increase in AATs with a $\beta T_{\mathrm{AAT}>0}$ ranging from 0.59–1.10, ST warming could vary from +2.5 °C at moist and vegetated depressions to +5.5 °C at dry rocky crests. The outcome of temperature increase in STs being greater, on average, than for AATs would require soils to dry first due to increase in AATs with high vapor pressure deficit in the soil increasing the soil-atmosphere temperature coupling. However, such a situation is unlikely in the Arctic, except at dry rocky crests, due to perennial snow packs acting as soil moisture inputs (Blankinship *et al* 2014). The buffering potential of STs is especially prominent under AAT ≤ 0 conditions, and in most parts of the landscape, as long as there is snow, the ST response would be highly limited. Accounting for snow distribution is thus of paramount importance to predict the buffering potential of the Arctic landscape according to STs, and thus might contribute to delay the negative impact of macroclimate warming on vegetation and wildlife redistribution (Bertrand *et al* 2011).

Our analyses only cover the factors controlling intra-annual soil-atmosphere ΔT and βT, which are unlikely to be constant over the years (Lenoir *et al* 2017). Instead, local environmental conditions related to snow, soil hydrological conditions and vegetation properties are expected to change due to climate warming (Tape *et al* 2006, Bintanja and Andry 2017). This limits our ability to assess the long-term buffering capacity of Arctic ecosystems, which would require longer time series ($\gg$ three years) of continuous measurements (Lenoir *et al* 2017). Main uncertainties in the anticipated changes are related to snow and soil moisture dynamics (Räisänen 2008, Pithan and Mauritsen 2014). Recent studies are in consensus that winter conditions (temperature, precipitation amount and phase) are expected to change the most dramatically under future climate change (Callaghan *et al* 2011, Räisänen and Eklund 2012, Bintanja and Andry 2017). Changes in snow conditions could lead to a highly non-linear feedback where a decrease in snow depth and an increase in days with AAT > 0 (here on average increasing by 88 days assuming +5 °C AAT warming) cause STs to be more strongly coupled with AATs (figure 5). This effect is especially pronounced in parts of the landscape with shallow snow accumulations where βT rapidly responds to small alterations in snow depth (Grundstein *et al* 2005). Changes in snow and associated ST variation (as seen in figure 4(*b*)) could thus have effects on physical processes through alterations of wind exposure and soil freezing. Previous studies have also indicated that winter soil thermal conditions have profound carry-over effect on multiple ecosystem properties (soil respiration, nutrient mineralization, carbon cycling and microbial activity) of the following growing season (Wipf *et al* 2009, Semenchuk *et al* 2016).

Synoptic temperature data from coarse-grained climatic grids does not capture the near-surface temperature conditions that are relevant for many abiotic and biotic processes (Graae *et al* 2012, Etzelmüller 2013, Potter *et al* 2013). Our results of intra-seasonal ΔT indicates that the absolute magnitude of this mismatch was on average >3 °C during our study period, exceeding 8 °C during the AAT$\leq$0 period. The insufficiency of contemporary climate data to describe local STs under future conditions (Williams and Jackson 2007) is further strengthened after considering the effects of βT on soil warming. The cascading effect of ΔT and βT implies that future microclimatic warming trajectories are likely to considerably differ from the ones that are based on coarse-grained climatic grids (Lenoir *et al* 2017). Here we demonstrate that changes in snow distribution are key to understanding the effects of climate warming in Artic ecosystems. However, it is important to highlight that even during the warm period, remarkable variations in βT within few meters were observed that could contribute to a non-uniform warming across the landscape. Therefore, Arctic ecosystems might be more or less directly affected by changes in atmospheric temperature than expected (e.g. in Post *et al* 2009, Pearson *et al* 2013), which may in turn modify current impact projections (in positive or negative ways), suggesting a need for re-assessment of the local rate of climate warming and associated impacts in Arctic regions.

Our findings are highly applicable across snow-dominated Arctic and alpine environments, and highlight the necessity to deploy continuous microclimatic monitoring of both soil and ambient air temperatures, and consideration of fine-scale environmental heterogeneity to support ecosystem impact modelling assessments.

Acknowledgments

J A and M L were funded by the Academy of Finland (project numbers 307761 and 286950). D S and A G obtained support from the Swiss National Science Foundation (grant: 1528661). Authors declare no competing financial interests. Underlying data which support the findings of this study are available from the corresponding author on request.

ORCID iDs

J Aalto https://orcid.org/0000-0001-6819-4911
D Scherrer https://orcid.org/0000-0001-9983-7510
J Lenoir https://orcid.org/0000-0003-0638-9582
A Guisan https://orcid.org/0000-0002-3998-4815
M Luoto https://orcid.org/0000-0001-6203-5143

References

Aalto J, le Roux P C and Luoto M 2013 Vegetation mediates ST and moisture in arctic-alpine environments *Arct. Antarct. Alpine Res.* **45** 429–39

Ashcroft M B and Gollan J R 2013 Moisture, thermal inertia, and the spatial distributions of near-surface soil and air temperatures: understanding factors that promote microrefugia *Agric. Forest Meteorol.* **176** 77–89

Bates D, Mächler M, Bolker B and Walker S 2014 Fitting linear mixed-effects models using lme4 (arXiv:1406.5823)

Bertrand R, Lenoir J, Piedallu C, Riofrío-Dillon G, De Ruffray P, Vidal C, Pierrat J C and Gégout J 2011 Changes in plant community composition lag behind climate warming in lowland forests *Nature* **479** 517–20

Billings W 1973 Arctic and alpine vegetations: similarities, differences, and susceptibility to disturbance *Bioscience* **23** 697–704

Bintanja R and Andry O 2017 Towards a rain-dominated Arctic *Nat. Clim. Change* **17** 263–7

Blankinship J C, Meadows M W, Lucas R G and Hart S C 2014 Snowmelt timing alters shallow but not deep soil moisture in the Sierra Nevada *Water Resour. Res.* **50** 1448–56

Blok D, Schaepman-Strub G, Bartholomeus H, Heijmans M M, Maximov T C and Berendse F 2011 The response of Arctic vegetation to the summer climate: relation between shrub cover, NDVI, surface albedo and temperature *Environ. Res. Lett.* **6** 035502

Bowman W D and Seastedt T R 2001 *Structure and Function of an Alpine Ecosystem: Niwot Ridge, Colorado* (Oxford: Oxford University Press)

Bruun H H, Moen J, Virtanen R, Grytnes J, Oksanen L and Angerbjörn A 2006 Effects of altitude and topography on species richness of vascular plants, bryophytes and lichens in alpine communities *J. Veg. Sci.* **17** 37–46

Callaghan T V, Johansson M, Brown R D, Groisman P Y, Labba N, Radionov V and Golubev V N 2011 The changing face of Arctic snow cover: a synthesis of observed and projected changes *AMBIO: J. Hum. Environ.* **40** 17–31

Dobrowski S Z 2011 A climatic basis for microrefugia: the influence of terrain on climate *Glob. Change Biol.* **17** 1022–35

Etzelmüller B 2013 Recent advances in mountain permafrost research *Permafrost Periglac. Process.* **24** 99–107

Fox J and Weisberg S 2011 *An R Companion to Applied Regression* (Thousand Oaks, CA: Sage Publishing)

French H M 2007 *The Periglacial Environment* (New York: Wiley)

Geiger R, Aron R H and Todhunter P 2009 *The Climate Near the Ground* (Rowman and Littlefield)

Gisnås K *et al* 2016 Permafrost map for Norway, Sweden and Finland *Permafrost Periglac. Process.* **28** 359–78

Graae B J *et al* 2018 Stay or go–how topographic complexity influences alpine plant population and community responses to climate change *Perspect. Plant Ecol. Evol. Syst.* **30** 41–50

Graae B J *et al* 2012 On the use of weather data in ecological studies along altitudinal and latitudinal gradients *Oikos* **121** 3–19

Grace J B 2006 *Structural equation Modeling and Natural Systems* (Cambridge: Cambridge University Press)

Graham E A, Rundel P W, Kaiser W, Lam Y, Stealey M and Yuen E M 2012 Fine-scale patterns of soil and plant surface temperatures in an alpine fellfield habitat, White Mountains, California *Arct. Antarc. Alpine Res.* **44** 288–95

Grundstein A, Todhunter P and Mote T 2005 Snowpack control over the thermal offset of air and STs in eastern North Dakota *Geophys. Res. Lett.* **32** L08503

IPCC 2013 Summary for policymakers *Climate Change 2013: The Physical Science Basis. Contribution of Working Group I to the Fifth Assessment Report of the Intergovernmental Panel on Climate Change* ed T F Stocker *et al* (Cambridge: Cambridge University Press) pp 3–29

King L and Seppälä M 1987 Permafrost thickness and distribution in Finnish Lapland—results of geoelectrical soundings *Polarforschung* **57** 127–47

Körner C 2003 *Alpine Plant Life: Functional Plant Ecology of High Mountain Ecosystems; with 47 Tables* (Berlin: Springer)

Lawrence D M and Swenson S C 2011 Permafrost response to increasing Arctic shrub abundance depends on the relative influence of shrubs on local soil cooling versus large-scale climate warming *Environ. Res. Lett.* **6** 045504

Lefcheck J S 2015 piecewiseSEM: Piecewise structural equation modelling in r for ecology, evolution, and systematics *Methods Ecol. Evol.* **7** 573–9

Lenoir J *et al* 2013 Local temperatures inferred from plant communities suggest strong spatial buffering of climate warming across northern Europe *Glob. Change Biol.* **19** 1470–81

Lenoir J, Hattab T and Pierre G 2017 Climatic microrefugia under anthropogenic climate change: implications for species redistribution *Ecography* **40** 253–66

Paradis M, Lévesque E and Boudreau S 2016 Greater effect of increasing shrub height on winter versus summer ST *Environ. Res. Lett.* **11** 085005

Patsiou T S, Conti E, Zimmermann N E, Theodoridis S and Randin C F 2014 Topo-climatic microrefugia explain the persistence of a rare endemic plant in the Alps during the last 21 millennia *Glob. Change Biol.* **20** 2286–300

Pearson R G, Phillips S J, Loranty M M, Beck P S, Damoulas T, Knight S and Goetz S J 2013 Shifts in Arctic vegetation and associated feedbacks under climate change *Nat. Clim. Change* **3** 673–7

Pecl G T *et al* 2017 Biodiversity redistribution under climate change: impacts on ecosystems and human well-being *Science* **355** eaai9214

Pirinen P, Simola H, Aalto J, Kaukoranta J, Karlsson P and Ruuhela R 2012 Tilastoja Suomen ilmastosta 1981–2010 (Raportteja - Rapporter - Reports 2012:1)

Pithan F and Mauritsen T 2014 Arctic amplification dominated by temperature feedbacks in contemporary climate models *Nat. Geosci.* **7** 181–4

Pollack H N, Smerdon J E and Van Keken P E 2005 Variable seasonal coupling between air and ground temperatures: a simple representation in terms of subsurface thermal diffusivity *Geophys. Res. Lett.* **32** L15405

Post E *et al* 2009 Ecological dynamics across the Arctic associated with recent climate change *Science* **325** 1355–8

Potter K A, Woods H A and Pincebourde S 2013 Microclimatic challenges in Globle Change Biology *Glob. Change Biol.* **19** 2932–9

le Roux P C, Aalto J and Luoto M 2013a Soil moisture's underestimated role in climate change impact modelling in low-energy systems *Glob. Change Biol.* **19** 2965–75

le Roux P C, Lenoir J, Pellissier L, Wisz M S and Luoto M 2013b Horizontal, but not vertical, biotic interactions affect fine-scale plant distribution patterns in a low-energy system *Ecology* **94** 671–82

le Roux P C and Luoto M 2014 Earth surface processes drive the richness, composition and occurrence of plant species in an arctic–alpine environment *J. Veg. Sci.* **25** 45–54

Räisänen J 2008 Warmer climate: less or more snow? *Clim. Dyn.* **30** 307–19

Räisänen J and Eklund J 2012 21st Century changes in snow climate in Northern Europe: a high-resolution view from ENSEMBLES regional climate models *Clim. Dyn.* **38** 2575–91

Rose J P and Malanson G P 2012 Microtopographic heterogeneity constrains alpine plant diversity, Glacier National Park, MT *Plant Ecol.* **213** 955–65

Saito M, Kato T and Tang Y 2009 Temperature controls ecosystem CO_2 exchange of an alpine meadow on the northeastern Tibetan Plateau *Glob. Change Biol.* **15** 221–8

Scherrer D and Körner C 2010 Infra-red thermometry of alpine landscapes challenges climatic warming projections *Glob. Change Biol.* **16** 2602–13

Scherrer D and Körner C 2011 Topographically controlled thermal-habitat differentiation buffers alpine plant diversity against climate warming *J. Biogeogr.* **38** 406–16

Semenchuk P R, Christiansen C T, Grogan P, Elberling B and Cooper E J 2016 Long-term experimentally deepened snow decreases growing-season respiration in a low-and high-arctic tundra ecosystem *J. Geophys. Res. Biogeosci.* **121** 1236–48

Starr G, Oberbauer S F and Ahlquist L E 2008 The photosynthetic response of Alaskan tundra plants to increased season length and soil warming *Arct. Antarct. Alpine Res.* **40** 181–91

Taka M, Aalto J, Virkanen J and Luoto M 2016 The direct and indirect effects of watershed land use and soil type on stream water metal concentrations *Water Resour. Res.* **52** 7711–25

Tape K, Sturm M and Racine C 2006 The evidence for shrub expansion in northern alaska and the pan-arctic *Glob. Change Biol.* **12** 686–702

Toms J D and Lesperance M L 2003 Piecewise regression: a tool for identifying ecological thresholds *Ecology* **84** 2034–41

William J W and Jackson S T 2007 Novel climates, no-analog communities, and ecological surprises *Front. Ecol. Environ.* **5** 475–82

Wipf S, Stoeckli V and Bebi P 2009 Winter climate change in alpine tundra: plant responses to changes in snow depth and snowmelt timing *Clim. Change* **94** 105–21

Wundram D, Pape R and Löffler J 2010 Alpine ST variability at multiple scales *Arct. Antarc. Alpine Res.* **42** 117–28